Slow dynamics of photospheric regions of the open magnetic field of the Sun, solar activity phenomena, substructure of the interplanetary medium and near-Earth disturbances of the early 23rd cycle:

2. The March–June 1997 events

K. G. Ivanov, A. V. Belov, A. F. Kharshiladze, and E. P. Romashets [1]

V. Bothmer [2]

P. J. Cargill [3]

I. S. Veselovskiy [4]

Short title: SLOW DYNAMICS OF PHOTOSPHERIC REGIONS

[1] Institute of Terrestrial Magnetism, Ionosphere, and Radio Wave Propagation, Troitsk, Moscow Region, Russia
[2] Max-Plank Institut fur Aeronomie, Katlenburg-Lindau, Germany
[3] Imperial College of Science, Technology, and Medicine, London, UK
[4] Moscow State University, Russia

Abstract. Slow (from one rotation to another) dynamics of the photospheric regions of the open magnetic field of the Sun (ORs), solar activity phenomena (coronal holes, active filaments, flares), subsector structure of the coronal field on the source surface, and near-Earth interplanetary medium are considered at the piece of the solar surface ~120 degree wide centered at the CL 150° Carrington latitude in the sequence of the CR 1920–CR 1923 Carrington rotations (March–June 1997). A special attention is paid to a prominent event of this period on 12–18 May 1997. It is demonstrated that in the coarse of the slow dynamics of ORs on the part of the Sun chosen, there was formed in the CR 1922 a specific configuration of ORs on the photosphere which generated a complicated structure of the magnetic field at the source surface and in the interplanetary field with a strong bow of the heliospheric current sheet (HCS) and a "joint" between HCS and the intersector boundary. A complicated solar activity complex was formed near this "joint", the complex consisting of a flare active region (AR), low-latitude coronal hole (CH), and active filament (ADF).

During CR 1920–CR 1922 there was observed a dynamical high-velocity flow which generated in CR 1921–CR 1922 a near-Earth MHD disturbance with three-phase temporal dynamics typical for the disturbances near HCS. The destabilization of the AR–CH–ADF–HCS complex in CR 1922, occurrence of a coronal mass ejection (CME) in AR, and the interaction between CME, HCS, ADF, and CH led to a significant modification of the recurrent high-velocity flow (appearance of the main shock wave and magnetic cloud, multiple crossings of HCS, velocity increase, and a "loading" of the flow by the active filament substance) and to a sharp increase of its geoefficiency. Possible scenarios of the 12–18 May 1997 events are discussed: a simple one with the magnetic cloud from AR 8038 [*Webb et al.,* 2000a] and a complicated one which includes a formation of the cloud due to the interactions in the activity complex with an HCS tiring-instability [*Kivelson and Khurana*, 1995] and its modeling by the heliospheric electrojet field [*Ivanov and Romashets*, 1999].

1. Introduction

There are arguments in the solar-terrestrial physics in favor of the statement that many interplanetary MHD-disturbances are generated by complicated solar sources, the latter being various combinations of coronal holes, filaments, flares, and active regions [*Bravo et al.*, 1998; *Burlaga et al.*, 1987; *Crooker and McAlister*, 1997; *Dryer and Smith*, 1987; *Gonzalez et al.*, 1996; *Gosling*, 1993; *Ivanov*, 1996, 1998; *Kahler*, 1991; *Mogilevsky et al.*, 1997]. In the complicated source concept, very perspective in our opinion is its representation as a large unstable configuration of the solar magnetoplasma in which coronal holes, filaments, and active regions are closely interrelated and are only specific components of this source (complex), characterizing its formation, destabilization, and decay [*Gosling*, 1993; *Mogilevsky et al.,* 1997].

There appear two fundamental problems concerning the phenomenology of such complexes: first, to study their dynamics at characteristic times of the order of a few solar rotations, second, studies of the interactions between its components, especially at the source destabilization phase leading to complicated interplanetary disturbances.

I has been shown recently that the activity complexes appear (disappear) in mutual collisions (reflections) of photospheric regions of the open magnetic field of the Sun [*Ivanov and Kharshiladze*, 2002; *Ivanov et al.*, 2001b]. As a result, we propose to use the dynamics of open regions as a convenient instrument for determination in advance of the tendencies leading to formation and destabilization of activity complexes including such determinations into the analysis of some prominent events of the solar-terrestrial physics. The analysis of the well-known disturbances of 5–11 January 1997 [*Ivanov et al.*, 2001a, 2002] is an example of such an approach. It was demonstrated in the above-cited papers that there was observed a convergence of open photospheric regions at least one rotation prior to the activity complex destabilization, that the filament-active region and coronal hole were the most active components of this complex, and that taking into account of

the interaction between them is important for explanation of the main characteristics and some peculiarities in the configuration, structure and dynamics of the interplanetary disturbance observed near the Earth. At the same time, the set of these characteristics and features is an experimental requirement which makes it possible to indicate perspective approaches to the MHD modeling of this disturbance.

Similar approach is used below to consider in detail the 12–18 May 1997 event. This event is interesting in particular due to the fact that in this event for the first time the Morton wave was registered in the extreme ultraviolet [*Thompson et al.*, 1998], a coronal halo was observed [*Plunkett et al.*, 1998; *Sheeley et al.,* 1999; *Webb et al.*, 2000a], a pair of transient coronal holes (dimmings) located symmetrically relative the neutral line of the active region magnetic field was formed [*Hudson et al.*, 1998; *Thompson et al.*, 1998], preflare sigmoid shape of the coronal arcs was observed [*Glover et al.*, 2000; *Hudson et al.*, 1998], the photospheric bases of the post-eruptive arc coincided almost exactly with the magnetic spots of the opposite polarity [*Thompson et al.*, 1998; *Webb et al.*, 2000a], small rapid (during the flare) and considerable slow (of about a day) variations of the magnetic flux in the active region were registered [*Lara et al.*, 2000], and the most intense magnetic storm of 1997 was observed [*Bruckner et al.*, 1998; *Ivanov and Romashets,* 1998]. Considering the data of the Wind/Waves radiophysical experiment, *Gopalswamy et al.* [2000] referred to this event as to a radio-rich event because there presented in it not only the meter and kilometer, but also deca- and hectometer radiobursts of type II.

Considering the data of this event, *Gibson and Low* [2000] proposed a model of the initial instability of the magnetoplasma configuration of the compact spheroid (spheromac) type.

Considerable attention has been paid also to the near-Earth interplanetary disturbance: to the cloud modeling [*Ivanov and Romashets*, 1999, *Watari et al.*, 2001; *Webb et al.*, 2000a, 2000b], to variations of the solar energetic particles [*Cane et al.*, 1998; *Lario*

et al., 2000; *Makela et al.*, 1998; *Mazur et al.*, 1998; *Sanderson et al.*, 1998; *Torsti et al.*, 1998] and two-direction super-thermal electron fluxes [*Shodhan et al.*, 2000]. Attention has been also drawn to the three-phase dynamics of the near-Earth disturbance (especially to the MHD structure of its preliminary (precursor) phase [*Ivanov and Petrov*, 1999; *Ivanov et al.*, 1999]) and to the ground-based variations of the galactic cosmic rays [*Munakata et al.*, 2000].

It is desirable to continue the studies of this event in the following directions:

First, on analogy with the 5–11 January 1997 event [*Ivanov et al.,* 2001a, 2002], to take into account the slow (from one rotation to another) dynamics of the photospheric regions of the open field, solar activity complexes and interplanetary medium structure.

Second, to pay attention to the fact that almost in all papers cited above the interpretation and modeling of the near-Earth disturbance is based on the consideration of only those solar events which had been formed in AR 8038 after the 1n(C.1.3) flare near the central meridian. The fact that these events could have been altered in interactions in the activity complex was never taken into account. Relating to this, we would note that the event have occurred in the vicinity of the heliospheric current sheet (HCS) [*Ivanov and Romashets*, 1999; *Sanderson et al.*, 1998] and that between the active region and HCS an active ($L = 12°$) and dense ($I = 2$) active filament of the ADF type was observed (Solar-Geophysical Data, Boulder, NN 637–640, 1998). Therefore, on the propagation path of the coronal mass ejection (CME) from the Sun to the Earth an interaction of CME with ADF and HCS should have occurred. Thus it is interesting to bear in mind that, though the kilometer radiobursts of the type II were observed by the Wind satellite almost permanently till the arrival of the forward shock wave to the Earth [http://lep694.gsfc.nasa.gov/waves/typeII], their intensity was very small [*Reiner et al.*, 1998], especially till about 1800 UT on 13 May. The latter fact makes it possible to assume that they were screened by the plasma sheet on HCS [*Ivanov and Romashets*, 2001]. Thus

the presence of the activity complex (AR + ADF + HCS) and the above-indicated interactions could be manifested in the structure and dynamics of the near-Earth disturbance, in particular, in the appearance of the disturbance preliminary phase and magnetic cloud closely related to HCS [*Ivanov and Petrov*, 1999; *Ivanov and Romashets*, 1999; *Ivanov et al.*, 1999].

Third, to pay attention to various approaches to modeling of the near-Earth magnetic cloud in this disturbance: it is either a field of the heliospheric electrojet on HCS [*Ivanov and Romashets,* 1999], or a field of a powerless cylinder (part of a toroidal configuration related to the bipolar group in AR) [*Watari et al.,* 2001; *Webb et al.*, 2000a].

Forth, to bear in mind that the problem of the plasma origin may be related to the problem of the magnetic cloud origin. For example, *Webb et al.* [2000a] paid attention to the fact that in this magnetic cloud neither "plasma density pulse" nor any sign of the filament substance were observed contrary to the magnetic cloud in the 10–11 January 1997 event [*Burlaga et al.*, 1998]. According to the *Hudson et al.* [1998] estimates based on the dimensions of "dimmings" in the soft X rays, the cloud contained only a small part of the total mass of CME. These observations contradict to the modeling of the initial configuration in which the filament substance was located within the cloud (magnetic bundle) [*Gibson and Low*, 2000]. It is possible that in this event the cloud is closely related (not only spatially but also by its origin) to HCS and presents an analog of rarefied plasmoids appearing in the magnetotail during the reconnection process [*Kivelson and Khurana,* 1995]. In favor of this assumption probably is the fact that there was no two-directional electron fluxes in the cloud [*Shodhan et al.,* 2000; *Webb et al.*, 2000a].

Fifth, to clarify the reason of the discrepancy between the directions of the magnetic axes of the bipolar group in AR to the Sun and of the magnetic cloud near the Earth. *Webb et al.* [2000a] suggested that to the moment of its arrival to the Earth orbit the cloud has turned around by $\sim 40^\circ$ and shifted southward by $\sim 30^\circ$ from its initial position such

that the cloud axis became located below the ecliptic plane. There is no such difficulty in the alternate model of cloud generation on HCS [*Ivanov and Romashets,* 1999].

The paper contains: section 2 "Initial data and Methods", section 3 dedicated to the dynamics of the photospheric open field, subsector structure of the coronal field and solar activity phenomena, section 4 dedicated to the dynamics of the subsector structure of the interplanetary medium, section 5 "The 12–16 May, 1997 events", and section 6 "Discussion".

2. Initial Data and Methods

To determine the spherical coefficients of the Gauss series in one of the versions of the solar magnetic field potential model with a source surface [*Kharshiladze and Ivanov*, 1994], the observations of the photospheric magnetic field at the Wilcox Solar Observatory [http://quake.Stanford.edu/*wso] are used. Then the open (going away into the interplanetary medium) lines of the magnetic field are projected from the source surface (a spherical surface with $r = 2.5R_{\odot}$ from the center of the Sun) onto the photosphere using the *Levine et al.* [1977] method. In the process of such modeling, the computer memorizes mutually-unambiguous relation between a particular photospheric region of the open field (OR) and the corresponding domain on the source surface. As a result, it becomes possible to obtain synoptic maps of the Sun in the Mercator projection. Combined on these maps are ensembles of photospheric ORs and the subsector structure of the solar magnetic field with the sector and intersector boundaries (Figures 1 and 2). Further, the following data were put onto these maps: the boundaries of the coronal holes in the FeXIV line observed at the Sacramento Peak Observatory, magnetic fields of the sunspot groups observed at the Kitt Peak Observatory, active filaments (Table 1), and flares (Solar-Geophysical Data, Boulder, NN 637–640, 1998). Then: 1) a piece of the

disk with the width $\Delta\Lambda = 150°$ centered at the Carrington longitude $\Lambda = 140°$ where the solar activity events responsible for the near-Earth disturbance on 14–16 May 1997 were observed; 2) slow (from one rotation to another) dynamics of the open regions, solar activity events, and the sector structure of the coronal field on the source surface were considered on this piece of the disc during four Carrington rotations (CR 1920–CR 1923: March–June 1997).

The data on the interplanetary magnetic field (IMF) and solar wind plasma obtained on board the Wind satellite (the leading scientists were P. Lepping and K. Ogilvie, http://cdaweb.gsfc.nasa.gov) obtained in the scope of the International Solar-Terrestrial Physics Program (ISTP) were used to study the dynamics of the subsector structure of the interplanetary medium and the correspondence of this dynamics to solar events. A special attention has been paid to the 14–16 May 1997 disturbance.

3. Photospheric Open Regions, Solar Activity, and the Field on the Source Surface

The structure, configuration, and dynamics of the photospheric open regions, solar activity events (coronal holes, filaments, and active regions), and coronal magnetic field (sector and intersector boundaries)on the source surface in the sequence of four Carrington rotations CR 1920–CR 1923 are considered below.

3.1. CR 1920, 12–23 March 1997 (Figure 1a)

The photospheric open field (closed circles) is mainly concentrated in the polar caps (at the heliolatitudes $|\Phi| \geq 70°$). The positive and negative polarity lines are located in the northern and southern hemispheres, respectively.

However, part of the open lines exits outside the polar caps to lower latitudes (the groups of larger circles designated as $+2$ and -1, -2 in the northern and southern hemispheres, respectively). Moreover, in the northern hemisphere there is a low-latitude photospheric open region designated as $+1$.

The distance between ORs of opposite polarity, $r > R_{\odot}$, manifests a remote interaction between these ORs which allows for formation of low-latitude coronal holes (thin curves) and active filaments (line segments),as well as for a deformation of the sector boundary on the source surface (solid curve) [*Ivanov et al.*, 2001b].

The coronal field on the source surface is mainly formed by the open lines emerging from the polar caps. Moreover,there are several subsectors ($+1$; $+2$; -1; -2) formed by the open lines going out from the corresponding open photospheric regions shown on the map by large black circles. The intersector boundaries on the source surface (the boundaries of subsectors) are shown by thin lines.

It is worth noting the following: 1) The helioprojection of the Earth passes through two low-latitude coronal holes formed by the open lines emerging from the photospheric polar regions (from the caps and OR $+2$ and -2). *Levine et al.* [1977] were the first to draw attention to such specific low-latitude holes. 2) There are several active filaments in the vicinity of the sector boundary. 3) There is no active regions (except one very small region near the joint of HCS and the -2 intersector boundary). During this rotation, a very durable (22–28 March) high-velocity flow was observed near the Earth with complicated profiles of the velocity V, concentration n, and temperature T, the profiles indicating to a loading of the flow by the filament substance.

3.2. CR 1921, 8–19 April 1997 (Figure 1c)

On 15 April the following changes happened in the ensemble of ORs on the piece of the solar surface considered: 1) in the northern hemisphere OR +2 disappeared, a high-latitude region was formed at the OR +1 meridian, and the OR +1 region itself expanded northward toward OR +3; 2) in the southern hemisphere OR −2 disappeared and OR −1 was shifted eastward, its area increasing significantly.

Interactions between ORs of the opposite polarity determined by the distance between the centers of OR +1 and OR −1 ($r > R_{\odot}$) still remains a remote one. The field on the source surface is still formed mainly be the open lines emerged form the polar caps. However, the Earth's helioprojection goes though the subsector structure of the coronal field formed by the open lines going out from the OR +1 and OR −1 midlatitude parts of the photosphere.

The sector boundary is in a considerable nonequilibrium in the sense that during the 8–11 April and 12–17 April periods it is formed by the oppositely directed open lines of the midlatitude OR +1 and southern polar cap, and OR −1 and the northern cap, respectively. As e result of this nonequilibrium, the sector boundary gets bows to the north and south from the equator, respectively.

It should be noted also that: 1) though the total area of the low-latitude coronal holes was reduced as compared to CR 1920, a small coronal hole in the vicinity of the joints of the sector and subsector boundaries is visually seen. Nevertheless, this coronal hole is still formed by the open lines going out from the OR −1 photospheric region located at higher latitude that the this hole; 2) below the subsector boundary of OR −1 there appeared a low-latitude active region 8032 of the new solar activity cycle. On 15 April at 1410 UT there occurred a solar flare of a moderate (maximum) optical ball SN(1N)/C1.0 in the point with the coordinates S23 E09 (Solar-Geophysical Data, Boulder, NN 637–640, 1998).

It is interesting that the position of this flare relative the equator and central meridian was almost mirror as compared to the 12 May flare (see the next section) responsible for the prominent near-Earth disturbance on 15 May 1997; 3) there was almost no filaments in the vicinity of the Earth's helioprojection.

During this rotation near the Earth, as well as in CR 1920, a high-velocity flow from the coronal hole was observed,the flow having shorter duration and relatively smooth profiles of V, n, and T.

3.3. CR 1922, 5–16 May 1997 (Figure 2a)

In the northern hemisphere there happened almost complete dissipation of OR +1, whereas OR +3 was shifted eastward. In the southern hemisphere there happened further shifting of OR −1 eastward and equatorward. The interaction between ORs still is remote and the subsector structure on the source surface stays almost unchangeable. The nonequilibrium of the sector structure is mainly conserved.

The most significant change of the activity complex as compared with CR 1921 was an appearance of an active filament and active region in the vicinity of the joint between the sector and intersector boundaries in addition to the coronal hole which existed in the previous rotations. In the active region in the N23 W09 point a flare 1n(C.1.3) occurred at 0445 UT on 12 May 1997 and initiated the solar-terrestrial disturbance on 12–16 May 1997. Thus, the very destabilization of the (A–AD–CH–HCS) activity complex formed near the joint of the sector and intersector boundaries between CD 1921 and CR 1922 became a cause of the corresponding disturbances on 14–16 May 1997.

Therefore, to create a qualitatively correct scenario and MHD model of this disturbance, one should take into account the entire complex of the solar activity and the influence of its components (coronal holes, filaments and heliospheric current sheet) on

generation and propagation of the shock wave, magnetic cloud, and solar and galactic cosmic rays, whereas in the majority of the papers dedicated to the 12–16 May 1997 event, only the sporadic phenomena related to AR 8038 were taken into account. The heliospheric current sheet was taken into account by *Sanderson et al.* [1998], the current sheet and active filament were taken into account by *Ivanov and Romashets* [1999] and *Ivanov and Petrov* [1999]. *Lario* [2000] noted that corresponding high-velocity flow measured by Ulysees on 19 May 1997 was recurrent. Till now nobody has considered the low-latitude coronal hole (Figure 2a) as one of the sources of the near-Earth disturbance.

3.4. CR 1923: 1–12 June 1997 (Figure 2c)

Comparing the CR 1922 and CR 1923 rotations, one can conclude that in the space between OR +3 and OR −1 there occurred a decay of the activity complex responsible for the 12–16 May 1997 disturbance. Actually: first, the active region with the bipolar group has disappeared, though on the place of the complex there are still observed two active filaments and a low-latitude coronal hole. Their mutual position became less compact and their geometric characteristics changed. This "remnants" of the complex still are located near the joint of the sector and intersector boundaries, but the former has a zero inclination relative the equator contrary to CR 1922.

It is possible that the decay of this complex is related to two events. First, to the energy loss in the May 1997 sporadic events. Second, to the decrease of the energy income into the interaction region of the pair of the OR +3 and OR −1 open regions. The latter suggestion is confirmed by a depletion of the OR +3 region area as compared with the two previous rotations.

4. Dynamics of the Near-Earth Interplanetary Medium

Now we consider the corresponding sequence of the states of the near-Earth interplanetary medium observed in the CR 1920 and CR 1923 rotations on board the Wind satellite (Figures 3–8). We would like to demonstrate that the formation, destabilization, and decay of the activity complex considered in section 3 are manifested in these disturbances.

4.1. Dynamics of the Solar Wind Velocity Profiles (Figure 3)

The wind velocity is characterized by a well pronounce dynamics. At the initial stage of the complex development (CR 1920) there is a complicated profile formed by a sequence of two flows. At the formation and destabilization stages (CR 1921–CR 1922) there is a high-velocity flow almost stable during two days in the duration, intensity and profile shape. At the decay phase (CR 1923) there is a stationary slow solar wind. It is worth noting that the V profiles in the CR 1921 and CR 1922 rotations are so similar that one can came to the conclusion on the absence of any influence of the known sporadic events of 12 May 1997 [*Hudson et al.*, 1998; *Plunkett et al.,* 1998; *Thompson et al.*, 1998; *Webb et al.*, 2000a, 2000b].

Evidently, this stability of the velocity profile is due to the fact that the dynamics of the solar wind velocity near the Earth was mainly governed by the dynamics of the low-latitude coronal holes responsible for this flow. Actually, in the beginning (CR 1920, Figure 1a) a sequence of two large holes was observed. However, the first one is formed by the open lines from the polar cap photosphere, whereas the second is screened from the Earth by the heliospheric current sheet. Probably this fact predetermined the low velocity in the first flow and the complicated profile of the velocity in the second flow. The maximum velocity in the second flow was caused by a break of the screening due to

the Earth crossing of the heliospheric current and entering the coronal hole. During the two following rotations (CR 1921 and CR 1922) the helioprojection of the Earth passed across the same coronal hole which was stable in its shape and position and formed by the open lines emerged from the midlatitude photosphere.

Thus the question arises, how the coronal mass ejection 12 of May 1997 influenced the velocity profile near the Earth? To answer this question we should pay attention to fine features of the velocity profile near the Earth in Figure 3. *Ivanov and Romashets* [1999] and *Ivanov and Petrov* [1999] paid attention to the fact that the near-Earth disturbance of 14–16 May 1997 was characterized by a three-phase time dynamics. A sequence of development (G), main (M), and recovery (R) phases and also its manifestation in all parameters of the solar wind plasma and IMF components are typical for this dynamics. Figure 3 confirms the presence of the three-phase dynamics in the velocity profiles observed during CR 1921 and CR 1922.

One should note a small difference in the May and April (CR 1922) profiles: 1) The development phase is better pronounced in April than in May. 2) The main phase starts from the SI flow surface in April and S_f forward shock wave in May. 3) The directions of the velocity changes are different during the main phase: there is a decrease in April soon after SI and a durable increase in May after S_f. 4) The flow is observed between the sector and one of the intersector (HCS and SB) boundaries in April and between two intersector boundaries in May.

These differences may be interpreted (see also the concentration and IMF profiles) as effects of a modification of the initial high-velocity flow observed during the CR 1921 rotation (April) and interactions in the (AR–CH–ADF–HCS) complex formed after the flow destabilization in May 1997. These effects were: 1) A formation of slow, dense, and cool heliospheric plasma layer because of the deceleration of the flow due to the ADF active filament on the HCS current sheet. 2) Generation of the shock wave both due to

some acceleration of the flow from the coronal hole induced by the energy input from CME of 12 May 1997 and to lowering of the threshold for the generation of a rapid magnetosonic shock wave while it was propagating though the dense and cold plasma of the active filament.

To interpret qualitatively the velocity profiles in CR 1921 and CR 1922 it is useful to take into account two factors, one accelerating and the other decelerating the flow. The acceleration could be caused by AR 8026 (S24 E09) and AR 8038 (N21 W09) (Solar-Geophysical Data, Boulder, NN 637–640, 1998) in which there were observed flares of the sn and 1n balls on 16 April and 12 May respectively. The deceleration could be due to the phenomena of "loading" of the high-velocity flows by the active filaments' substance (Table 1).

4.2. Dynamics of the Profiles of the Solar Wind Proton Concentration (Figure 4)

The variations of N in the high-velocity flow before and after the solar activity complex destabilization (CR 1921 and CR 1922) are the most interesting.

These profiles are similar, but there are also considerable differences between them. First, a strong and durable increase of the concentration in the head part of the flow was observed during both rotations. However in CR 1921 it was a rather smooth compact variation with a sharp increase and smooth decrease, almost entirely located on HCS (between the sector and subsector boundaries, the latter in this rotation almost completely coinciding with the flow surface). As to the increase in CR 1922, it was a more irregular grow with a sharp depletion of the concentration at the front boundary of the cloud. The increase consisted of two parts: the increase during the development phase of the disturbance (in front of HCS and shock front)and the increase in the shock layer in front

of the magnetic cloud.

Second, the concentration within the cloud is depleted in both rotations. However the concentration profile in CR 1921 is almost flat ($N \sim$ const), whereas this profile in CR 1922 is irregular with a decrease of N in the magnetic cloud and a train of high-amplitude fluctuations upward along the flow from the cloud.

This feature of the N profile in CR 1922 may be qualitatively explained by the presence of relatively dense heliospheric plasma sheet formed in the interaction of ADF and HCS [*Ivanov and Romashets*, 1999]. The latter (as it has been shown above, see Figure 2a) was adjacent to the low-latitude coronal hole. The N profile in the previous rotation CR 1921 was more smooth since in this rotation, though a hole in the vicinity of HCS was observed, there was no such powerful filament as ADF (Figure 1c).

Ivanov [2001] proposed to call such increase of the density within high-velocity flows as a "loading" by active filaments' substance. Moreover the high-velocity flow in question was "loaded" by magnetic cloud as well. It should be noted that *Webb et al.* [2000a] indicated that this cloud is located in the front part of the high-velocity flow, though they did nor discuss the nature of this flow; it was presumed that the flow was a posteruptive flow being part of the halo-like CME formed in AO 8038.

4.3. Dynamics of IMF. The Magnetic Cloud on the Heliospheric Current Sheet

At the stage of the activity complex development (CR 1920 and CR 1921), the near-Earth satellites should have been located mainly in the IMF negative sector (Figure 1). This statement is confirmed by the IMF measurements at the Wind satellite (Figures 5–8). Actually, the field almost all the time is directed sunward ($B_x > 0$) and westward ($B_y < 0$). Only during some short periods the IMF direction changes to the opposite. The

magnetic fluctuation level is high, the fact additionally indicating that the satellite orbit is close to HCS and that the latter is unstable. The destabilization of the solar activity complex (CR 1922) initiated a near-Earth disturbance during which the Wind satellite exited the positive sector and (after triple crossing of the sector boundary at 0038 UT, 0518 UT, and 0950 UT on 15 May) entered first the magnetic cloud (0951 UT) and then, after exiting the cloud (∼2330 UT on 15 May) almost till 0300 UT of 17 May was located mainly in the IMF negative sector ($B_x > 0$, $B_y < 0$). Therefore, the magnetic cloud in the 15 May disturbance was located at the heliospheric current sheet and its nature might have been closely related to the magnetic field of this layer, the field of the heliospheric electrojet [*Ivanov and Romashets*, 1999]. The fact that the cloud was close to HCS was not taken into account in the known publications [*Watari et al.*, 2001; *Webb et al.*, 2000b] dedicated to modeling of this cloud by solving the inverse problem in which the geometric characteristics of a powerless cylinder configuration are determined from the experimental profiles of the B_x, B_y, and B_z components.

Moreover, it was assumed in the above-mentioned publications that the cloud was a magnetic bundle, a part of the coronal mass ejection from AR 8038.

Below we consider in detail various properties of the solar-interplanetary disturbance of 12–16 May 1997 including the nature and modeling of the magnetic cloud.

5. Near-Earth Disturbances of the Interplanetary Medium of 14–18 May 1997

The dynamics, structure, and configuration of the near-Earth interplanetary disturbance of 14–18 May 1997 are considered in this section in detail. The aim of the consideration is to reveal characteristics of this disturbance which are detected experimentally and can be used for testing various MHD models oriented to this very disturbances.

5.1. Structure and Configuration of the Near-Earth Disturbance

The structure of this disturbance in the interplanetary medium near the Earth was considered by *Ivanov and Petrov* [1999], *Ivanov and Romashets* [1999], *Ivanov et al.* [1999], and *Webb et al.* [2000a]. Three phases of this disturbance were detected: preliminary (the development phase G) (∼0810 UT on 14 May–∼0110 UT on 15 May), main phase M (from 0110 UT on 15 May to ∼0300 UT on 16 May), and recovery phase R (after 0300 UT on 16 May). It was shown that the G phase is a monotonic variations of the IMF components modulated by almost continuous train of nonlinear Alfvén waves and rotational ruptures [*Ivanov and Petrov*, 1999; *Ivanov et al.*, 1999]. It was suggested that the G phase is a preliminary result of the interaction between ADF and HCS contained in the activity complex in question (Figure 2a). Further on, the sporadic coronal mass ejection CME from AR 8038 becomes involved into the interaction and the main phase of the disturbance occurs. Namely during the main phase of the disturbance the shock wave and magnetic cloud are observed. However one should bear in mind that the shock wave and cloud are interacting with HCS and slow dense solar wind from the active filament ADF [*Ivanov and Romashets,* 1999]. Moreover, it was found (Figure 2a) that the high-velocity flow from the low-latitude coronal hole CH also becomes involved into interaction, so as a result we have in this disturbance a complicated CME–CH–ADF–HCS interaction. This fact should be taken into account in interpretation and modeling of this disturbance.

Below we consider in more detail the structure and configuration of the main phase of this disturbance.

Table 2 shows the results of determination of the φ_N and θ_N showing the direction of the prevailing propagation of nonlinear waves and ruptures (RDs) during the development phase of the disturbance. Also presented in Table 2 are: normals to the heliospheric current sheet HCS1, HCS2, HCS3, and HCS4, to the forward shock wave S_f, and to the

magnetic cloud boundary in the entrance R_I and exit R_{II} points.

The scatter matrix method is used to determine these directions; the coordinates are solar-ecliptic. The normals to S_f and R_I determined by *Berdichevsky et al.* [2000] and calculated by us from the magnetic cloud geometric characteristics obtained by *Webb et al.* [2000a], respectively, are marked by asterisks.

It follows from Table 2 that: 1) The disturbance propagates westward in its front part (1500 UT on 14 May–1000 UT on 15 May). 2) The conclusion of *Webb et al.* [2000a] that the magnetic cloud axis lies slightly below the ecliptic plane ($\theta_N > 0$ for the normal to R_I and $\theta_N < 0$ for the normal to R_I), is confirmed. A triple crossing of HCS (Figure 9) is observed, the θ_N sign changing which makes possible a schematic presentation of the disturbance geometry shown in Figure 10. 4) After the first and third crossings of HCS, there were observed a forward shock front S_f and the magnetic cloud front boundary R_I, which formed closely-located pairs of the raptures HCS1–S_f and HCS2–R_I (Figures 9 and 10).

These results confirm the assumption that, since the complicated solar source of the disturbance included a piece of the heliospheric current sheet(Figure 2a), this fact should have been manifested in the structure of the near-Earth disturbance. Certainly, an explicit MHD model should reproduce all the sequence of the structural elements shown in Table 2.

Concluding, we note that the observed distance of the forward shock wave from the front point of the cloud was in this disturbance $\sim 1.3 \times 10^{12}$ cm which (under the Mach number $M = 2.1$ [*Berdichevsky et al.*, 2000]) is very close to the theoretical value for a cloud with a shape of a circular cylinder [*Belotserkovskiy*, 1957]. However the normals to S_f and R_I are directed southward and northward, respectively (Table 2) which provides difficulties in connecting S_f to the magnetic cloud.

5.2. Forbush-Effect in the Galactic Cosmic Rays

Figure 11 shows variations of the density A_0 and anisotropy A_{xy} of the rigid ($\sim$10 GV) component of the galactic cosmic rays obtained by the global survey method from the neutron monitors network. The variations consist of a gradual preincrease ($\sim$1500–2400 UT on 14 May), more sharp fluctuations of the decrease and increase ($\sim$0000–1000 UT on 15 May), the "main" depletion ($\sim$1000–2400 UT on 15 May), a small smooth fluctuation of the increase-decrease (0000–0600 UT on 16 May) and further slow recovery.

The amplitude of the effect ($\sim$1–1.5%) is anomalously small from the point of view of statistical relations with the interplanetary medium characteristics [*Belov et al.*, 2001]. For example, the expected values of the amplitude for the disturbance of 15 May 1997 ($V_{\max} = 500$ km s^{-1}, $B_{\max} = 25$ nT) is

$$\Delta A_0 \cong \frac{V_{\max}}{400}\,\frac{B_{\max}}{5} \cong 6\%$$

which is by a factor of 4.5 higher than the observed amplitude.

The temporal behavior of the amplitude is unusual since large-scale Fluctuations of GCR with the amplitude comparable to that of the "main" depletion has been observed both before and after the Forbush decrease.

Thus the Forbush effect is anomalous by its amplitude and unusual by its shape. The galactic cosmic ray (GCR) variations were compared to the MHD structure of the disturbance (Figures 9 and 10, Table 2) and led to the following conclusions: 1) The preincrease was observed in the negative IMF sector from the moment of the sharp decrease of the propagation direction of the nonlinear MHD waves and raptures (RD) to the moment of crossing HCS1, entering the IMF positive sector, and arrival of the shock front. 2) The sharp fluctuations of the increase, decrease, and again increase of A_0 almost coincided with the moments of the HCS1, HCS2, and HCS3 crossings of the heliospheric current

sheet, respectively, and were observed within the positive, negative, and again positive IMF sectors. 3) The "main" depletion was observed within the magnetic cloud ($R_I - R_{II}$).

The nature of the Forbush effect being closely related to the MHD structure of the near-Earth disturbance, is nevertheless still obscure.

The preincrease has the most clear interpretation as a typical event caused by the reflection and acceleration of particles at the shock front [*Dorman et al.*, 1970; *Ruffolo*, 1999; *Ruffolo et al.*, 1999].

For the model with an exponential decrease of A_0 upward the flow from S_f [*Ruffolo*, 1999] one can write:

$$\Delta A_0 = B + C \exp(kZ)$$

where B and C are constants, Z is the coordinate perpendicular to the front, k is a spatial scale of the preincrease (equal to D/U in the theory and evaluated in the experiment as $V_{sf}\ \tau$ where D, U, V_{sf}, and τ are the diffusion coefficient, the solar wind velocity in the shock front coordinate system and along the magnetic field, and the duration of the preincrease. In the event in question: $V_{sf} = 380$ km s^{-1}, $\tau = 12$ h, $k^{-1} = 1.5 \times 10^{12}$ cm, $D \simeq 3.5 \times 10^{19}$ cm^2 s^{-1}, and the transport path of particles with rigidity 10 GV $\lambda_{\rm II} = 3D/C \cong 3.5 \times 10^{12}$ cm. Moreover, $\Delta A_0 \simeq 1\%$ in this event (Figure 11) and the ratio of the tangential components of the magnetic field at the shock front is $B_{\tau 2)}/B_{\tau 1} \cong 4$ and agrees by a factor of 2 with the theoretical model of the preincrease [*Ruffolo*, 1999].

Still more difficult is the problem of interpretation of the GCR variations after the shock front passage. In general, one can conclude that these variations are due to the GCR interaction with the "crimped" HCS and magnetic cloud. A complete answer requires a knowledge on how the specific MHD disturbance structure has occurred. In general it is clear that it was formed as a result of the interaction with the HCS of the high-velocity flow

activated by CME from AR 8038 (see subsections 4.1–4.3). However a specific scenario of the formation of this structure still is obscure. One of the possibilities is to assume that the entire complicated structure of the MHD disturbance, including the "crimped" HCS and magnetic cloud, has been formed in the interaction of the activated high-velocity flow with HCS. This scenario is close to the one suggested earlier by *Ivanov and Romashets* [1999]. In the second version, the "crimped" HCS (but not the magnetic cloud)and corresponding fluctuations of GCR could have appeared in a collision with HCS of the magnetic cloud which has come from AR 8038. It is a modification of the *Webb et al.* [2000a] scenario in which HCS was not taken into account.

Thus unusual shape of the Forbush effect provides no arguments in favor of this or that hypothesis of the magnetic cloud origin.

At the same time, the properties of the Forbush variations found above and their relation to the MHD disturbance confirm a need to take into account the SME interaction with HCS while interpreting and modeling this disturbance.

The anomalously small amplitude of the Forbush effect also can not be a serious argument in favor or against any of the above-described hypotheses, though we think that this amplitude is more consistent with the model of the cloud formation on HCS. Relating to this, we emphasize that the "main" depletion of A_0 in the magnetic cloud (Figure 11) looks in this event as a normal decrease typical for the entire IMF positive sector. Actually, if one takes into account the sequence of three GCR decreases in the positive sector (the fluctuation behind S_f, the "main" depletion in the magnetic cloud, and the decrease after ~0400 UT on 16 May), than the "main" depletion has an intermediate value by the amplitude which indicate to a recovery of A_0 after the strongest decrease up to 1.5% in the sharp fluctuation behind the shock front.

To chose the hypothesis of the magnetic cloud origin, it would have been useful to consider in detail the variations of all the components of the anisotropy vector A_1.

Figure 11 shows the amplitudes of its components in the ecliptic plane A_{xy}. Within the cloud the amplitudes fall down to the minimum value at the nearest distance from the cloud axis.

In this event a considerable component $A_z \simeq 1\%$ directed northward was observed during the entire period of the cloud passage. Thus, one can make a preliminary conclusion that the data on the anisotropy vector variations are in favor of the hypothesis of the cloud formation on HCS, for example as a result of the mechanism which is proposed to explain formation of plasmoids in the magnetospheric tail [*Kivelson and Khurana*, 1995]: reconnection under a tiring-instability in the neutral layer.

The Forbush-effects of this disturbance were studied also in the integral ($E >$ 50 MeV) GCR flux on the basis of the observations at the SOHO satellite [*Makela et al.*, 1998] and in the ultra-relativistic part of the spectra on the basis of the data of the muon telescope network [*Munakata et al.*, 2000].

5.3. Radiobursts of Type II

This event is considered as a rare radio-rich event [*Gopalswamy et al.*, 2000] because of the presence in it together with the meter and kilometer radiobursts also of the deka- and hectometer radiobursts. According to the observations on board the Wind satellite [http://lep694.gsfc.nasa.gov/waves] there is no smooth transition between these wave ranges, whereas in the interplanetary medium the burst is weak and discontinuous [*Reiner et al.*, 1998], the fact allowing us to assume that it was screened by the heliospheric plasma layer [*Ivanov and Romashets,* 2001].

The weak radioburst at the frequency $\sim f_0 \sim 150$ kHz occurred in the interplanetary medium about 1800 UT on 13 May and lasted with some variations of the spectrum and small interruptions till ~0300 UT on 14 May. In the interval between 0300 and 0300:30 UT

a rapid decrease of the frequency down to $f_1 \sim 90$ kHz was observed with a transition to a very narrow emission band. These variations in the spectrum may be interpreted as a crossing by the shock front of a sharp boundary from more dense and inhomogeneous medium to less dense and more homogeneous medium. (If we estimate the density change approximately as the ratio of the frequencies squared, we obtain the density decreases by approximately a factor of 2.5). For example, the above fact might have been interpreted as an arrival of the shock wave into the vicinity of the heliospheric current layer or rarefied magnetic cloud.

6. Discussion

Below we briefly discuss the results of the papers in the following topics: solar sources, near-Earth disturbances, solar-interplanetary phenomena, and modeling. The accent is made upon the particular results and problems of the study of the 12–18 May 1997 disturbance.

6.1. Solar Sources

Analyzing the complex of solar, interplanetary and near-Earth data we show in this paper that: 1) the active complex AR(sf)–CH–ADF–HCS, i.e. a complex solar source, was a cause of the near-Earth disturbance; 2) this active complex was formed near the "joint" of the sector and intersector boundaries of the model coronal magnetic field on the source surface as a result of slow dynamics of the photospheric regions of the open field of the Sun.

These results specify ideas on the solar source of the near-Earth disturbance as compared both with the publications in which only the active region AR 8038 with the *sf* flare and small active filaments in this region is taken into account (for example, *Webb et*

al. [2000b]), and with the *Ivanov and Romashets* [1999] paper in which the low-latitude coronal hole CH in the Fe XIV line was not taken into account.

Certainly, in the source (especially on the Sun) the most pronounced were the sporadic phenomena in AR 8038 (flare, Morton wave, CME) [*Hudson et al.*, 1998; *Plunkett et al.*, 1998; *Sheeley et al.*, 1999; *Thompson et al.*, 1998; *Webb et al.*, 2000b], however the input of these sporadic events into the near-Earth disturbance, in our mind, needs specification. Also the input into this disturbance of the interactions of SME with HCS, ADF, and CH should be taken into account. This particular event confirms the tendency (which has been formed during the recent decade) to interpret the majority of near-Earth disturbances as complicated events with inputs from complex solar sources [*Bravo et al.,* 1998; *Crooker and McAlister*, 1997; *Gonzalez et al.*, 1996; *Ivanov*, 1996]. According to the terminology suggested by *Ivanov* [1998], the 12–18 May 1997 disturbance was a flare–hole–filament–strimmer one.

This event is the third in a series the events studied in which a complex solar source is formed near the joint of the sector and intersector boundaries as a result of slow dynamics of the photospheric regions OR of the open solar field. In two other cases, in July 2000 [*Ivanov and Kharshiladze*, 2002] and January 1997 [*Ivanov et al.*, 2002] this fact was also emphasized. The tendency of activity complex to appear in the interaction region of ORs in the vicinity of sector and intersector boundaries [*Ivanov et al.*, 2001b], in our opinion, agrees with the results which indicate to a frequent appearance of CME at the intersector chains of coronal streamers [*Eselevich,* 1995; *Fainshtein*, 1997; *Hundhausen,* 1993].

The problem of the interactions in a complex source which may begin on the Sun and be continued in the interplanetary medium till the arrival to the Earth orbit, is very important. In this event the source consist of closely located AR, ADF, HCS, and CH, and so one could expect a manifestation of these interactions in the data of solar observations.

One of such interactions (AR–HCS–CH) could, in our opinion, be manifested in the

strong nonhomogeniety of the UV-radiation front which propagated over the entire solar disc with the Morton wave after the flare at 0443 UT on 12 May (Figure 2 in *Thompson et al.* [1998]). The latter authors noted only the increase in the emission and deceleration of the part of the front propagated northward, the fact being interpreted as an interaction of the shock wave with the north polar coronal hole. To complete, we compare Figure 2 from the *Thompson et al.* [1998] paper to Figure 2a of this paper and note that the largest irregularity in the emission (at 0450–0507 UT in the solar disk segment with $\Delta\Phi = 15°$, $\Delta\Lambda \simeq 20°$ and with the center at $\Phi = S5$, $\Lambda = W10$ from the flare meridian) almost completely covers the nearest to the Earth piece of HCS and the low-latitude CH which were part of the considered solar activity complex. This fact may be considered as an indication to an interaction of the shock wave with HCS and CH and to possible consequences of this interaction (besides the nonhomogeneous front of the UV radiation, those are also a formation of the magnetic bundle [*Gosling*, 1990; *Marubashi*, 1986] and of the HCS bow [*Wu and Dryer*, 1997]). This fact has not been taken into account in the MHD modeling of the Morton wave in the 12 May 1997 event. Figure 4 in the *Wu et al.* [2001] paper shows a comparison of the observations of the UV-radiation front [*Thompson et al.*, 1998] with the simulation results obtained under an assumption that the wave propagates in a medium with constant values of the density and temperature. As a result, the model front was homogeneous in all directions, including south-westward from the flare where the filament was located and a strong nonhomogeniety of the emission was observed. Finally, modeling a near-Earth disturbance, various alternatives should be considered of the formation of the magnetic cloud observed in the near-Earth disturbance [*Ivanov and Romashets*, 1999; *Makela et al.*, 1998; *Shodhan et al.*, 2000; *Watari et al.*, 2001; *Webb et al.,* 2000a, 2000b].

6.2. Near-Earth Disturbance

The near-Earth disturbances in the interplanetary medium on 14–16 May 1997 have been studied relatively weakly. The main attention has been paid to the MHD structure of the development phase of this disturbance [*Ivanov and Petrov*, 1999; *Ivanov et al.*, 1999], to local models of the magnetic clouds based on the ideas on the heliospheric electrojet field [*Ivanov and Romashets*, 1999] and on powerless field of a circular cylinder [*Watari et al.*, 2001; *Webb et al.*, 2000a], and also to the energetic particles [*Lario et al.,* 2000; *Makela et al.*, 1998; *Munakata et al.*, 2000; *Sanderson et al.,* 1998; *Shodhan et al.*, 2000; *Torsti et al.*, 1998].

It was assumed in the very beginning that this is a complicated disturbance from the complicated solar source with the flare, active filament and heliospheric current sheet [*Ivanov and Romashets*, 1999]. Later it was found (see sections 3–4) that it is not enough, since we are dealing with a recurrent high-velocity flow form a low-latitude coronal hole modified by the interactions in the AR–CH–ADF–HCS complex.

However, this fact does not exclude the question on the magnetic cloud origin in May 1997. It was shown in section 4 that the cloud was observed on HCS and so, besides the assumption that the cloud is a magnetic bundle, a part of CME from AR 8038 [*Gibson and Low,* 2000; *Webb et al.*, 2000a], it is desirable to bear in mind a possibility of generation of this cloud on HCS in the AR–CH–ADF–HCS complex by one of the mechanisms discussed in literature [*Gosling,* 1990; *Ivanov and Romashets*, 1999; *Kivelson and Khurana*, 1995; *Marubashi*, 1986; *Wu and Dryer*, 1997].

It is significant that, contrary to the 5–12 January 1997 events [*Ivanov et al.*, 2002], the determination of the normal to the cloud at the point of the entrance of the Wind satellite based on the geometric characteristics of a circular cylinder cloud in the *Webb et al.* [2000a] and *Watari et al.* [2001] calculations does not contradict the determination

of the normal by the scatter matrix method (Table 2). The cloud was neither strongly deformed nor strongly compressed, so the usual method of looking for configuration characteristics from the IMF components [*Burlaga,* 1988] is applicable to this cloud. The absence of a strong "density pulse" at the cloud rear wall and a Forbush increase of the GCR intensity within the cloud in the May event provides an additional confirmation of the assumption on a significantly different degree of compression of these clouds. The latter means that the May cloud should not be classified as a "super-expanding" cloud in which strong currents at the cloud boundary and deviations of the cloud shape from a cylinder should be taken into account [*Cargill et al.,* 2000; *Schmidt and Cargill*, 2001].

However, the position of the forward shock wave relative the front boundary of the cloud does not agree completely with the *Berdichevsky et al.* [2000] assumption that this is a deflected wave under a quasi-stationary flowing around with the Mach number $M = 2$. Actually, the normals to S_f and R_I diverge by $\sim 30°$ and are directed southward and northward, respectively. This means that during 8.5 hours between the crossings of S_f and R_I either the magnetic cloud turned to the south by a jump, or the wave changed its direction sharply while crossing HCS, or the cloud was not a generator of this wave.

There is one more "configuration" problem of relation of this cloud to a solar source. It looks like the following. *Webb et al.* [2000a] came to the conclusion that the cloud axis lies southward from the Earth below the ecliptic plane. Our determinations by different methods confirm this conclusion (Table 2). To agree the position of AR 8038 (N23 W09) as a possible source of this cloud with the position of the cloud axis one has to suggest that on its way from the Sun to the Earth the cloud was shifted southward almost by 30° and turned anticlockwise by 50–60° [*Webb et al.*, 2000a]. No particular evidences have been presented in favor of these suggestions except the reference to the rotation in the proper direction of the active filament from this AR. In the cloud models oriented to its origin on HCS (for example, in the model with the heliospheric electrojet [*Ivanov and*

Romashets, 1999]) the problem is easily eliminated since in the cloud observation moment HCS in this event was located southward from the Earth (see section 4).

If we discuss the hypothesis on the shift and turn of the cloud, we should pay attention to the following: 1) the CME-halo was more bright at the north and east than at the south and west [*Plunkett et al.*, 1998]; 2) some role was played by the interaction of the coronal shock wave with the HCS and CH located south-westward (this fact is manifested by the strong nonhomogeniety of the Morton wave (Figure 2 in *Thompson et al.* [1998]); this interaction, in particular, could have generated the reflected wave pushing the cloud from AR 8038 north-east; 3) one has to agree the spheromack model by *Gibson and Low* [2000] applied by these authors to AR 8038 AR in which the magnetic bundle (cloud) in the initial position was located along the neutral line of AR, whereas in the interpretation of *Webb et al.* [2000a] the initial position of the cloud was perpendicular to this line.

What was happening with this disturbance on the way from the Sun to the Earth one can only assume on the basis of the Forbush effects observed at the network of neutron monitors (see subsection 5.2) and muon telescopes [*Munakata et al.*, 2000] and also on board the SOHO satellite [*Makela et al.*, 1998]. These were observations of the particles with the rigidity of about 10 GV, 16–890 GV, and the integral flux of the particles with the rigidity above 50 MeV, respectively. It would be interesting to compare these results to the measurements in the spectrum of the kilometer emission of type II (see subsection 5.3).

The first thing we would like to point out to is an astonishing coincidence of the moments of the integral GCR flux preincrease observed on board SOHO [*Makela et al.*, 1998] with the moment of the appearance of a weak kilometer radioburst of type II (see subsection 5.3). This coincidence occurred at about 1800 UT on 13 May and may be interpreted as a very quick reaction of GCR at the distance of $\sim$0.5 AU from the Sun. Further on, till the arrival of the shock front to the Earth, the particle density increased by about 4%. Contrary to the Forbush effects in the ultrarelativistic part of the spectrum, the

density variations in the integral flux behaved in agreement with the statistically mean characteristics [*Belov et al.*, 2001]: a two-step (at the shock wave and in the magnetic cloud) decrease was observed and the expected value of the decrease amplitude (∼7%) was reached.

It is worth also noting that the beginning of the rigid GCR preincrease (∼1500 UT on 14 May, see Figure 11) was close to the time of the sharp change of the propagation direction of the nonlinear MHD oscillations (RDs in Table 2). Not long before that (0300–0400 UT on 14 May) a sharp reconstruction of the spectrum of the radioburst of type II occurred according to the observations on board the Wind satellite (see subsection 5.3). It is possible that these events indicate to the fact that the interplanetary wave shortly before its arrival to the Earth took pert in the interaction with large-scale irregularities of the interplanetary medium (magnetic cloud, HCS), however the exact physical sense of these interactions is still obscure.

An explanation of the cloud spirality may present a difficulty in the hypothesis of the cloud formation on HCS. In this case (according to the spirality rules for the solar cycle [*Bothmer and Schwenn,* 1998]) it was a left-spiral SEN cloud [*Webb et al.,* 2000a]. The cloud spirality near the Earth is easily explained by the magnetic field spirality of the bipolar group in AO 8038 [*Webb et al.*, 2000a], however it is not clear which should be the spirality of the cloud generated on HCS. In relation to this we note that the same problem with the spirality appears in *Mulligan et al.* [2001] who have found a cyclic variation in the positive correlation between the directions of the magnetic clouds axes and the HCS inclination to the equator plane. In the event in question, the magnetic cloud could have been formed at the part of HCS formed by remote interactions of the pair of open regions +3/-1 (Figure 2a), which have the same longitudinal shift as the sunspots of the bipolar group in AR 8038. Probably, solving this problem, one would be able to explain the spirality of the magnetic cloud on 15 May 1997 without denying the assumption on its

generation on HCS.

6.3. Scenario and Model of the Disturbance

This event is presented above as consisting of a slow phase of gradual formation of the activity complex and rapid phase of this complex destabilization with a strong disturbance in the space between the Sun and the Earth.

Obviously, currently there is not enough either experimental data not theoretical concepts which would make it possible to describe and model the entire chain of the events unambiguously and in detail. The most problematic still stays the description and explanation of the events during the slow phase. It is suggested [*Ivanov et al.*, 2001b] that the photospheric regions of the modeled magnetic field of the Sun together with large-scale background magnetic fields [*Bumba and Howard*, 1965] are a result and manifestation of giant modes of the convective instability [*Fox et al.*, 1998; *Simon and Weis*, 1968; *Wilson*, 1987, 1992; *Wilson et al.,* 1990; *Yoshimaru*, 1971], the interactions between them generating solar activity complexes. This view on the origin and role of the open magnetic field of the Sun is an alternate hypothesis on generation of the open field in the active solar regions [*Leigton,* 1964; *Wang et al.*, 2000]. Not rising a discussion on this fundamental problem, we would like to draw attention to the fact that (as has been shown in subsections 3.2 and 3.3) the appearance of the relatively separated open regions OR -1, $+2$, and $+3$ (Figures 1 and 2) and their tendency to a convergence preceded by almost one rotation the appearance of AR 8026 and 8038 and formation of the activity complex.

One more perspective approach to the interpretation of the dynamics of the photospheric regions of the open magnetic field of the Sun could be based on the concept of the Rossbi waves generated in the convective zone of the Sun and having the characteristic linear dimensions close to those of OR ($\sim 0.5R_{\odot}$) and a similar life-time (about 10 solar

rotations) [*Gilman,* 1969; *Tikhomolov and Mordvinov,* 1997].

The rapid phase scenario has more reliable and various experimental backgrounds than the slow phase scenario and makes some elements of modeling possible. It is mainly true for the events near the Sun and Earth. The data and ideas on what has been happening in the outer corona and interplanetary state still are limited and controversial.

In the scenario of the rapid phase which started on 12 May 1997 with sporadic events in AR 8038 [*Gopalswamy et al.*, 2000; *Hudson et al.*, 1998; *Plunkett et al.*, 1998; *Thompson et al.*, 1998; *Webb et al.*, 2000a, 2000b], it is assumed (see sections 3 and 4) that in the vicinity of AR 8038 AR and the helioprojection of the Earth there were located an active filament, part of the heliospheric current, and low-latitude coronal hole, all of them forming a united activity complex (Figure 2a).

Because of that, the sporadic disturbances formed in AR 8038 should have interacted with the above-indicated structural formations and the results of this interactions could have been manifested: in the strong inhomogeneity of the Morton wave front (see subsection 6.1) in the vicinity of the photosphere; in deca- and hectometer radioemission in the outer corona; in the sharp changes of the spectrum of the kilometer radioburst of type II (see subsection 5.3); in multiple crossings of HCS associated with the forward shock wave and magnetic cloud in the near-Earth environment; and in the anomalous Forbush effect in the MHD and GCR precursors of the disturbance (see subsections 5.1–5.2).

Certainly, the observations by *Gopalswamy et al.* [2000], *Hudson et al.* [1998], *Lara et al.* [2000], *Plunkett et al.* [1998], *Sheeley et al.* [1999], *Thompson et al.* [1998], and *Webb et al.* [2000a, 2000b] quite definitely show that AR 8038 was a source of the coronal mass ejection with the shock wave, magnetic cloud, ejection of a small filament, and posteruptive flow from the transient coronal holes. So one can assume that near the Earth was observed the same CME which had started from AR, if on the way to the Earth the cloud had shifted southward by almost 30° and turned around the longitudinal axis

by $\sim 45°$ [*Webb et al.*, 2000a].

The above-mentioned condition is, in our opinion, a weakest point of this scenario. Moreover neither the indicated above complicated complex of solar sources nor possible interactions and their consequences, especially in the near-Earth space, are taken into account in this scenario. Nevertheless, the scenario worth further study both, due to the direct relation to the observed properties of AR 8038 (the comparison of magnetic clouds in AR and in the magnetic cloud, cloud spirality according to the Bothmer and Rusta rule), and to the fact that the interactions and detailed features of the near-Earth disturbance found in this paper partially are able to be agreed with the *Webb et al.* [2000a] scenario. For example, if the consequences of the HCS collision with the magnetic cloud from AR were observed near the Earth, then one can consider as a result of this collision the multiple crossings of HCS in front of the front cloud boundary accompanied by large-amplitude fluctuations of the MHD parameters and GCR intensity (Figures 3–11).

A different scenario of these disturbances is known in which the complexity of the source was taken into account, possible interactions were discussed and it was suggested that the magnetic cloud was originated on HCS and may be presented as a heliospheric electrojet field [*Ivanov and Romashets*, 1999].

Taking into account the results of this study, this scenario may be presented in the following way. 1) On 12 May CME (the forward wave, magnetic cloud, posteruptive flow) starts from AR 8038, the south-western flank immediately interacting with ADF, HCS, and CH, this fact being manifested in the strong inhomogeniety of the Morton wave front [*Thompson et al.*, 1998] and occurrence of the deca- and hectometer radiobursts of type II [*Gopalswamy et al.,* 2000]. 2) A new magnetic cloud (an analog of a plasmoid in the magnetotail [*Kivelson and Khurana*, 1995]) is born near the Sun in the CME–HCS interaction act and is captured into the high-velocity flow from the low-latitude coronal hole CH loaded by the substance of the active filament ADF. 3) The forward shock wave

attenuates strongly, a return wave is formed, the magnetic cloud is pushed out of AR north-eastward. This facts are manifested by the almost complete disappearance of the II-type radiobursts [*Reiner et al.,* 1998] (see subsection 5.3) and a high intensity of the halo in its north-eastern part [*Plunkett et al.*, 1998]. 4) The posteruptive flow from AR overtake the slower "loaded" high-velocity flow from CH and accelerates it with formation of a shock wave in the region of the interaction of these flows. These facts are confirmed by the occurrence of the kilometer radioburst of type II at about 1800 UT on 13 May and correspond to the *Gopalswamy et al.* [1998] hypothesis on generation of kilometer radiobursts in two-flow interaction acts. 5) At ∼0300 UT on 14 May the newly generated wave reaches the rear wall of the magnetic cloud and enters it (that is confirmed by the sharp change of the spectrum of the radioburst of type II, see subsection 5.3), compresses and accelerates the cloud. 6) Subsequently, the acceleration of the cloud associated with HCS leads to oscillations ("crimping") of HCS (Figure 10) with a formation of a magnetic "mirror" responsible for the preincrease of GCR (Figure 11) and GCR fluctuations in front of the front boundary of the cloud.

The problem of the near-Earth cloud origin still stays under discussion, however it seems necessary to take into account the complicated source and interactions in a qualitative scenario of the 12–16 May 1997 disturbances to formulate a set of experimental limitations to the results of MHD modeling of such simple (at the first sight) events of solar-terrestrial physics.

7. Conclusion

Applied to the solar-interplanetary disturbance of 12–18 May 1997, a possibility is demonstrated to study complicated solar sources, structure, configuration, and dynamics of near-Earth disturbances using slow dynamics of the photospheric regions of the open

lines of the magnetic field of the Sun and a broad complex of solar observations and measurements in the interplanetary medium.

Is shown that: 1) The compact activity complex formed in April–May 1997 in the vicinity of the "joint" between the sector and intersector boundaries of the magnetic field on the source surface was a cause of the disturbance in question; 2) the complex included also an active region, active filament outside this region, and coronal hole; 3) the complex generated in the interplanetary medium a high-velocity magnetoplasma flow with the life-time of about 4 solar rotations (from the birth to the decay); 4) an interplanetary disturbance with the three-phase temporal dynamics typical for the disturbances in the vicinity of the heliospheric current sheet was observed in April–May 1997 near the Earth; 5) the destabilization of the 12 May 1997 complex led to a significant modification of the near-Earth disturbance: to the appearance of a forward shock wave and magnetic cloud, to the multiple crossings of the heliospheric current sheet and to the flow acceleration; 6) the close relation of the magnetic cloud to the heliospheric current layer, its geometric characteristics, and anomalously low amplitude of the Forbush decrease make possible an assumption that the magnetic cloud have been formed as a result of a reconnection of the magnetic field in the neutral layer of the heliospheric current layer.

Acknowledgments. The authors are grateful to R. Lepping, K. Ogilvie, and the CDAWeb group for the data of IMF and plasma measurements on board the Wind satellite, V. Kaiser for the data on the radiobursts of type II obtained in the Wind/waves experiment, T. Hoeksema for the data of the measurements of the photospheric magnetic field on board WSO, A. I. Zavoykina for her help in preparation of the paper. This work was supported by EU/INTAS-ESA (project 99-00-727) and the Russian Federation Program "Astronomy".

References

Belov, A. V., et al., What causes Forbush effects and what are they related to?, *Izv. Ros. Akad. Nauk, Ser. Fiz., 65*(3), 373, 2001.

Belotserkovskiy, O. M., Flowing around of a circular cylinder with a leaving shock wave, *Dokl. Akad. Nauk SSSR, 113*(3), 509, 1957.

Berdichevsky, D. B., A. Sabo, R. P. Vinas, and F. Mariani, Interplanetary fast shocks and associated drivers observed through the 23th solar minimum by Wind over its first 2.5 years, *J. Geophys. Res., 105*(A12), 27,289, 2000.

Bothmer, V., and R. Schwenn, The structure and origin of magnetic clouds in the solar wind, *Ann. Geophys., 16*(1), 1, 1998.

Bravo, S., X. Blanco-Cano, and E. Nikiforova, Different types of coronal mass ejections at minimum and maximum of solar activity and their relation to magnetic field evolution, *Sol. Phys., 180*(1/2), 461, 1998.

Bruckner, G. E., et al., Geomagnetic storms caused by coronal mass ejections (CMEs): March 1996 through June 1997, *Geophys. Res. Lett., 25*(15), 9019, 1998.

Bumba, V., and R. Howard, Large-scale distribution of solar magnetic fields, *Astrophys. J., 141*(4), 1502, 1965.

Burlaga, L. F., Magnetic clouds, and force-free fields with constant alpha, *J. Geophys. Res., 93*, 7217, 1988.

Burlaga, L. F., K. W. Behannon, and L. W. Klein, Compound streams, magnetic clouds, and major magnetic storms, *J. Geophys. Res., 92,* 5725, 1987.

Burlaga, L. F., et al., A magnetic cloud containing prominence material: January 1997, *J. Geophys. Res., 103*(1), 277, 1998.

Cane, H. V., I. G. Richardson, and O. C. St. Cyr, The interplanetary events of January–May 1997, as inferred from energetic particle data, and their relationship with solar

events, *Geophys. Res. Lett., 25*(14), 2517, 1998.

Cargill, P. J., J. Schmidt, D. S. Spicer, and S. T. Zalezhak, Magnetic structure of over-expanding coronal mass ejections. Numerical models, *J. Geophys. Res., 105*, 7509, 2000.

Crooker, N. U., and A. N. McAlister, Transients associated with recurrent storms, *J. Geophys. Res., 102*(A7), 14,041, 1997.

Dorman, L. I., N. S. Kaminer, and E. V. Kebuladze, Intensity increase of the cosmic rays prior to a Forbush decrease and strong shock waves in the interplanetary medium, *Izv. Akad. Nauk SSSR, Ser. Fiz., 34*(11), 2360, 1970.

Dryer, M., and Z. K. Smith, MHD simulation of multiple interplanetary disturbances during STIP interval VII (August 1979), in *Solar Maximum Analysis*, edited by V. E. Stepanov and V. N. Obridko, VNU Science Press, Utrecht, p. 369, 1987.

Eselevich, V. G., New results on the site of initiation of coronal mass ejections, *Geophys. Res. Lett., 22*(20), 2681, 1995.

Fainshtein, V. G., An investigation of solar factors governing coronal mass ejections characteristics, *Sol. Phys., 174*(1/2), 413, 1997.

Fox, P., P. McIntosh, and P. R. Wilson, Coronal holes and polar field reversal, *Sol. Phys., 177*(2), 375, 1998.

Gibson, S. E., and B. C. Low, Three-dimensional and twisted: An MHD interpretation of on-disk observational characteristics of coronal mass ejections, *J. Geophys. Res., 105*(A8), 18,187, 2000

Gilman, P. A., A Rossby-wave dynamo for the Sun, II, *Sol. Phys., 9*(1), 3, 1969.

Glover, A., N. D. Runs, L. K. Harra, and F. L. Culhane, The onset and association of CMEs with sigmoidal arcs, *Geophys. Res. Lett., 27*(14), 2161, 2000.

Gonzalez, W. D., et al., Coronal hole-active region-current sheet (CHARCS) association with intense interplanetary and geomagnetic storms, *Geophys. Res. Lett., 23*(19), 2577,

1996.

Gopalswamy, N., et al., Origin of coronal and interplanetary shocks: A new look with WIND spacecraft data, *J. Geophys. Res., 103*(1), 307, 1998.

Gopalswamy, N., et al., Radio-rich solar eruptive events, *Geophys. Res. Lett., 27*(8), 1200, 2000.

Gosling, F. T., Coronal mass ejections and magnetic flux ropes in interplanetary space, in *Physical of Magnetic Flux Ropes, Geophys. Monogr. Ser.*, edited by C. T. Russell, E. R. Prist, and L. C. Lee, AGU, Washington, D.C., v. 58, p. 330, 1990.

Gosling, J. T., The solar flare myth, *J. Geophys. Res., 98*, 18,937, 1993.

Hudson, H. S., J. R. Lemen, O. C. St. Cyr, A. C. Sterling, and D. F. Webb, X ray coronal changes during halo coronal mass ejections, *Geophys. Res. Lett., 25*(14), 2481, 1998.

Hundhausen, A. F., The sizes and locations of coronal mass ejections, *J. Geophys. Res., 98*(12), 13,177, 1993.

Ivanov, K. G., Solar sources of the interplanetary plasma streams on the Earth's orbit, *Geomagn. Aeron., 36*(2), 158, 1996.

Ivanov, K. G., The loading of a coronal hole with an active filament: Influence on the dynamics and structure of near-Earth disturbances, *Geomagn. Aeron., 41*(1), 1, 2001.

Ivanov, K. G., and A. F. Kharshiladze, Slow dynamics of open field lines as indicator of subphotospheric interactions, its relation to solar activity phenomena and near-earth disturbances. 2. The March–September 1999 events, *Geomagn. Aeron., 42*(2), 2002 (in press).

Ivanov, K. G., and V. G. Petrov, MHD structure of the precursors of interplanetary and geomagnetic disturbances, *Geomagn. Aeron., 39*(4), 403, 1999.

Ivanov, K. G., and E. P. Romashets, Prominent 1997 ISTP Phenomena. Workshop Present Achievement and Future Opportunities of ISTP and GEM, Yosemite, USA, 27, 1998.

Ivanov, K. G., and E. P. Romashets, Flare-filament–streamer interplanetary disturbances, *Geomagn. Aeron., 39* (2), 135, 1999.

Ivanov, K. G., and E. P. Romashets, Heliospheric current sheet effect on propagation of type II interplanetary radio bursts from coronal mass ejections, *Radio Sci., 36* (6), 1739, 2001.

Ivanov, K. G., E. P. Romashets, and V. G. Petrov, The wave vectors of nonlinear Alfvén waves at the growth phase of a flare-filament–streamer flow of interplanetary magnetoplasma, *Geomagn. Aeron., 39* (5), 539, 1999.

Ivanov, K. G., V. Bothmer, P. Cargill, A. F. Kharshiladze, E. P. Romashets, and I. S. Veselovsky, Subsector structure of the interplanetary space, SOLSPA 2001 Euroconference: Solar Cycle and Space Weather, Vico Equense, Italy, *ESA SP Ser.*, v. SP-477, p. 35, 2001a.

Ivanov, K. G., V. Bothmer, P. Cargill, A. F. Kharshiladze, E. P. Romashets, and I. S. Veselovsky, Slow dynamics of photospheric regions of open solar magnetic field, solar activity, substructure of the interplanetary space and near-Earth disturbances at beginning of 23-th solar cycle: 2. December 1996–February 1997 events, *IJGA*, 2002 (submit).

Ivanov, K. G., A. F. Kharshiladze, and A. N. Mel'nik, Slow dynamics of the open field lines as an indicator of underphotospheric interactions, its relation to solar activity events and near-Earth disturbances: 1. The July–October 1999 events, *Geomagn. Aeron., 41* (6), 1, 2001b.

Kahler, S., Coronal mass ejections and streamers associated with the new cycle activity regions at solar minimum, *Astrophys. J., 378*, 398, 1991.

Kharshiladze, A. F., and K. G. Ivanov, Spherical harmonic analysis of the solar magnetic field, *Geomagn. Aeron., 34* (4), 450, 1994.

Kivelson, M. G., and K. K. Khurana, Models of flux ropes imbedded in a Harris neutral

sheet, *J. Geophys. Res., 100*(12), 23,637, 1995.

Lara, A., N. Gopalswamy, and G. DeForest, Change on photospheric magnetic flux during CMEs, *Geophys. Res. Lett., 27*(10), 1435, 2000.

Lario, D., et al., Energetic protons observed at 1 and 5 AU. 1. January–September 1997, *J. Geophys. Res., 105*(A8), 18,235, 2000.

Leigton, R. B., Transport of magnetic fields on the Sun, *Astrophys. J., 140*(4), 1547, 1964.

Levine, R. H., M. D. Altschuler, and J. W. Harley, Solar sources of interplanetary magnetic field and solar wind, *J. Geophys. Res., 82,* 1061, 1977.

Makela, P., J. Torsti, M. Teittinen, et al., Observation of galactic cosmic ray modulation during Earth directed coronal mass ejections, *Geophys. Res. Lett., 25*(15), 2951, 1998.

Marubashi, K., Structure of the interplanetary magnetic clouds and their solar origins, *Adv. Space Res., 6*(6), 33, 1986.

Mazur, J. E., et al., Solar energetic particles inside magnetic clouds observed with the Wind spacecraft, *Geophys. Res. Lett., 25*(14), 2521, 1998.

Mogilevsky, E. T., V. N. Obridko, and B. D. Shelting, Large-scale magnetic field structures and coronal holes on the Sun, *Sol. Phys., 176*(1), 107, 1997.

Mulligan, T., et al., Inversion studies of magnetic cloud structure at 0.7 AU. Solar cycle variation, *Geophys. Res. Lett., 28*(5), 891, 2001.

Munakata, K., et al., Precursors of geomagnetic storms observed by the muon detector network, *J. Geophys. Res., 105*(A12), 27,457, 2000.

Plunkett, S. P., B. J. Thompson, R. A. Howard, D. J. Michels, O. C. St. Cyr, S. J. Tappin, R. Schwenn, and R. L. Lamy, LASCO observations of an Earth-directed coronal mass ejection on May 12, 1997, *Geophys. Res. Lett., 25*(14), 2477, 1998.

Reiner, M. J., M. L. Kaiser, J. Fainberg, and R. G. Stone, A new methods for studying remote type II radio emission from coronal mass ejection-driver shocks, *J. Geophys.*

Res., 103(A12), 29,651, 1998.

Ruffolo, D., Transport and acceleration of energetic charged particles near an oblique shock, *Astrophys. J., 515*(P2), 787, 1999.

Ruffolo, D., J. W. Biber, P. Evenson, and R. Pyle, Precursors to Forbush decreases and space weather predictions, *Proceedings of 26th International Cosmic Ray Conference*, v. 6, p. 440, 1999.

Sanderson, T. R., R. P. Lin, D. E. Larson, M. P. McCarthy, G. K. Parks, J. M. Bosqued, N. Lormant, K. Ogilvie, R. P. Lepping, A. Szabo, A. J. Lazarus, J. T. Steinberg, and J. T. Hoeksema, Wind observation of the influence of the Sun's magnetic field on the interplanetary medium at 1 AU, *J. Geophys. Res., 103*(A8), 17,235, 1998.

Schmidt, J., and P. J. Cargill, Magnetic cloud evolution in two-speed solar wind, *J. Geophys. Res., 106*(4), 8283, 2001.

Sheeley, N. R., J. H. Walters, Y.-M. Wang, and R. A. Howard, Continuous tracking of coronal outflows: Two kinds of coronal mass ejections, *J. Geophys. Res., 104*(A11), 24,739, 1999.

Shodhan, S., et al., Counterstreaming electrons in magnetic clouds, *J. Geophys. Res., 105*(A12), 27,261, 2000.

Simon, G. W., and N. O. Weiss, Supergranules and the hydrogen convection zone, *Z. Astrophys., 69*(6), 435, 1968.

Thompson, B. J., S. P. Plunkett, J. B. Gurman, J. S. Newmark, O. C. St. Cyr, and D. J. Michels, SOHO/EIT observations of an Earth-directed coronal mass ejection on May, 12, 1997, *Geophys. Res. Lett., 25*(14), 245, 1998.

Tikhomolov, E., and V. Mordvinov, Rossby fortices in the layer between convection zone and radiative interior, *Sol. Phys., 172*(1), 196, 1997.

Torsti, J., A. Antila, L. Kocharov, P. Makela, E. Rihonen, T. Sahla, M. Teittinen, E. Valtonen, T. Laitinen, and R. Vainio, Energetic ($\sim$1 to 50 MeV) protons associated with

Earth-directed coronal mass ejections, *Geophys. Res. Lett., 25*(14), 22,525, 1998.

Wang, Y. M., N. R. Sheeley, and J. Lean, Understanding the evolution of the Sun's open magnetic flux, *Geophys. Res. Lett., 27*(5), 621, 2000.

Watari, S., T. Watanabe, and K. Marubashi, Soft X-ray solar activity associated with interplanetary magnetic flux ropes, *Sol. Phys., 202*(2), 363, 2001.

Webb, D. F., E. W. Cliver, N. U. Crooker, O. C. St. Cyr, and B. J. Thompson, Relations hip of halo coronal mass ejections, magnetic clouds, and magnetic storms, *J. Geophys. Res., 107*(A4), 7491, 2000b.

Webb, D. F., R. P. Lepping, L. F. Burlaga, and C. E. DeForest, The origin and development of the May 1997 magnetic cloud, *J. Geophys. Res., 105*(A12), 27,251, 2000a.

Wilson, P. R., Solar rotation and giant celles, *Sol. Phys., 110*(1), 59, 1987.

Wilson, P. R., The reversal of the solar magnetic fields, *Sol. Phys., 138*(1), 11, 1992.

Wilson, P. R., P. S. McIntosh, and H. B. Snodgrass, The reversal of the solar polar magnetic fields, *Sol. Phys., 127*(1), 1, 1990.

Wu, C. C., and M. Dryer, Three-dimensional MHD simulation of IMF changes at 1 AU caused by a simulated solar disturbances and a titled heliospheric current/plasma sheet, *Sol. Phys., 173*(2), 391, 1997.

Wu, S. T., H. Zheng, S. Wang, B. J. Thompson, S. Plunkett, X. P. Zhao, and M. Dryer, Three-dimensional numerical simulation of MHD-waves observed by the Extreme Ultraviolet Imaging Telescope, *J. Geophys. Res., 106*(11), 25,089, 2001.

Yoshimaru, H., Complexes of activity of the solar cycle and very large-scale convection, *Sol. Phys., 18*(3), 417, 1971.

K. G. Ivanov, A. V. Belov, A. F. Kharshiladze, and E. P. Romashets, Institute of Terrestrial Magnetism, Ionosphere, and Radio Wave Propagation, Troitsk, Moscow

Region, Russia. ()

V. Bothmer, Max-Plank Institut fur Aeronomie, Katlenburg-Lindau, Germany

P. J. Cargill, Imperial College of Science, Technology, and Medicine, London, UK

I. S. Veselovskiy, Moscow State University, Russia

(Received 16 May 2002)

Table 1. Active Filaments

CR	Date	Type	Φ, grad	Λ, grad	L, grad	I
1920	12 March 1997	DSF	3 N	18 E	6	2
	14 March 1997	DSD	4 S	14 W		
	18 March 1997	AFS	10 S	12 W		
	20 March 1997	DSD	4 S	0 E	3	
	21 March 1997	DSF	42 S	31 E	8	2
1921	10 April 1997	ADF	15 N	14 W	7	1
	10 April 1997	ADF	27 S	14 W	11	1
	14 April 1997	AFS	23 S	23 E		
	15 April 1997	ADF	23 S	5 E	5	1
	15 April 1997	ADF	22 S	13 E	3	3
	16 April 1997	DSF	22 S	4 E	3	3
1922	6 May 1997	DSF	31 S	19 E	5	2
	8 May 1997	ADF	32 S	9 W		
	10 May 1997	ADF	14 N	15 E	12	2
	12 May 1997	DSF	32 S	29 E	5	1
	12 May 1997	ADF	23 N	9 W	4	1
1923	1 June 1997	ADF	21 N	13 E	8	1
	3 June 1997	AFS	5 N	10 E	1	
	3 June 1997	DSF	30 S	7 E	7	1
	4 June 1997	ADF	33 S	3 W	10	1
	5 June 1997	DSF	35 S	17 W	8	2
	6 June 1997	DSF	34 S	19 W	7	2

Table 2. Directions (the Solar-Ecliptic Coordinates) of the Propagation of Alfvén Waves (RDs), Normals to the Crossings of the Heliospheric Current (HCS), Forward Shock Wave (Sf), and Cloud Boundaries (R_I for the Entrance and R_{II} for the Exit)

Date	UT	Type	φ_N, grad	θ_N, grad
14 May 1997	0800–1500	RDs	140	−20
14 May 1997	1500–2400	RDs	230	−20
15 May 1997	0038	HCS1	219	23
15 May 1997	0115	S_f	207	−16
15 May 1997	0115	S_f	208*	−19*
15 May 1997	0518	HCS2	225	−23
15 May 1997	0950:30	HCS3	192	31
15 May 1997	0951:15	R_I	211	17
15 May 1997		R_I	192*	11*
15 May 1997	2325	R_{II}	173	−12
17 May 1997	∼0200	HCS4		

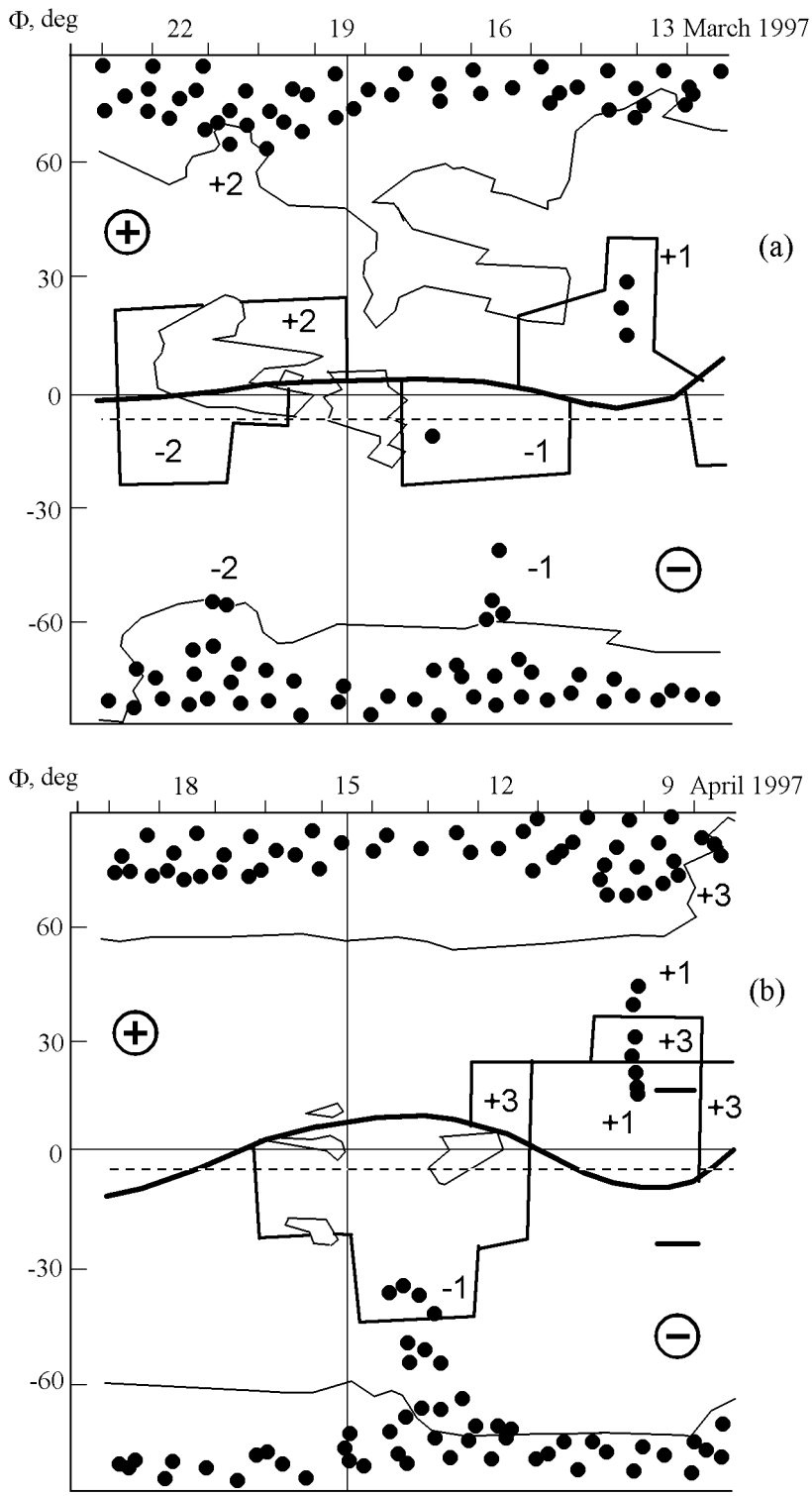

Figure 1. Photospheric regions of the open lines of the magnetic field of the Sun +1, +2, −1, −2 (black small circles), corresponding subsectors of the field on the source surface (polygons), solar activity phenomena: coronal holes with the boundaries shown by smooth curves, active filaments (line segments), active regions (black-and-white figures), and flares (crosses) in the CR 1920 (a) and CR 1921 (b) rotations. The dashed line shows the trajectory of the Earth's helioprojection.

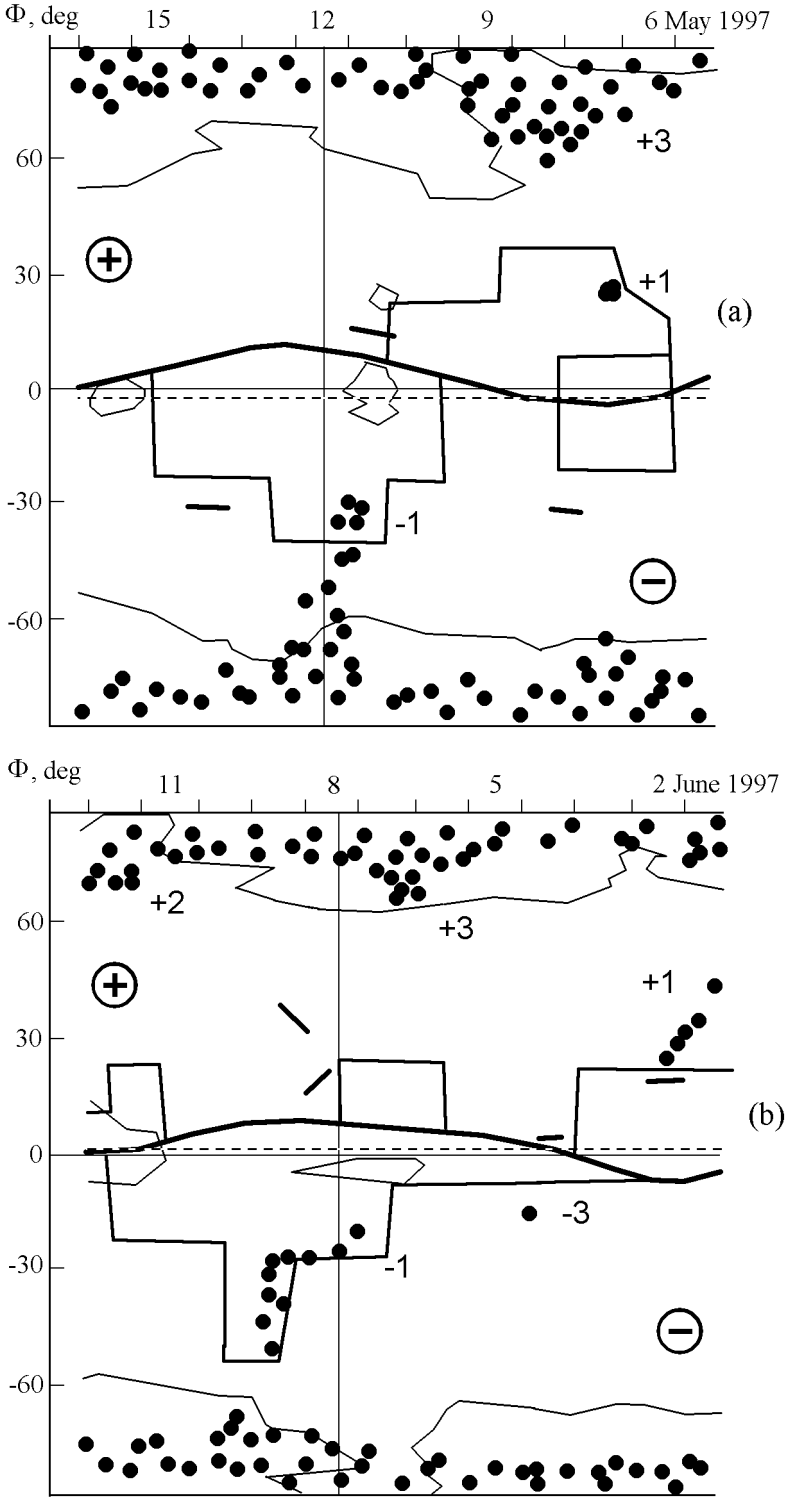

Figure 2. The same as in Figure 1 but for the CR 1922 (a) and CR 1923 (b) rotations.

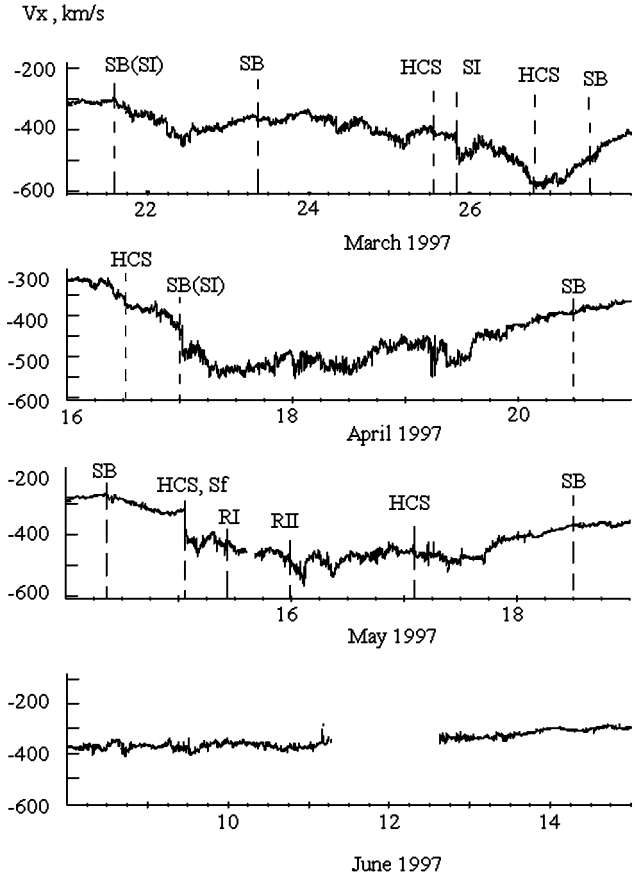

Figure 3. Dynamics of the solar-ecliptic V_x component of the solar wind according to the measurements on board the Wind satellite (courtesy of K. Ogilvie and GDA Web team) in the sequence of CR 1920–CR 1923 (from top to bottom). HCS, SB, SI, S_f, R_I, and R_{II} are the sector and subsector boundaries, flow surface, forward shock wave, and front and rear boundaries of the magnetic cloud, respectively.

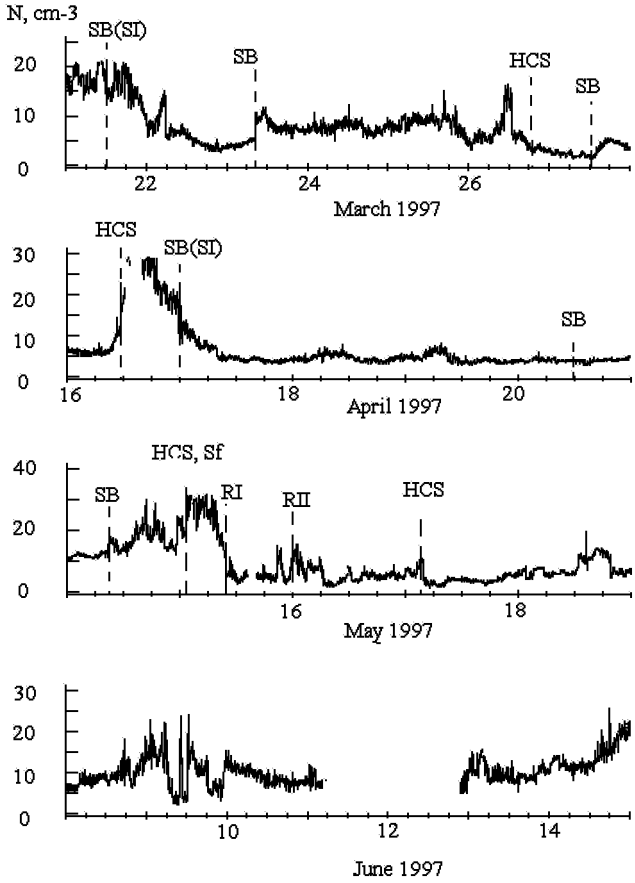

Figure 4. Dynamics of the solar wind protons concentration (the designations are the same as in Figure 3).

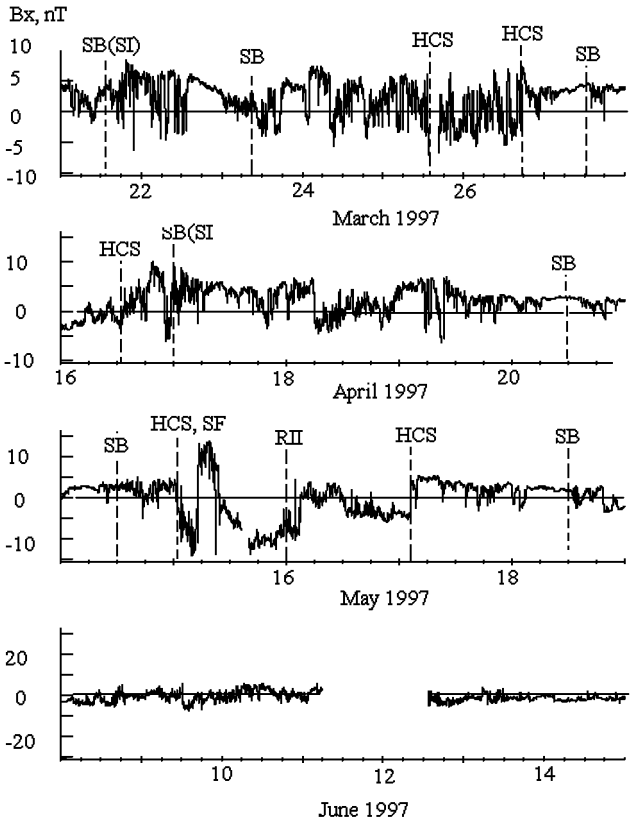

Figure 5. Dynamics of the B_x component of the interplanetary magnetic field according to the measurements on board the Wind satellite (courtesy of R. Lepping and CDA Web team) The designations are the same as in Figure 3.

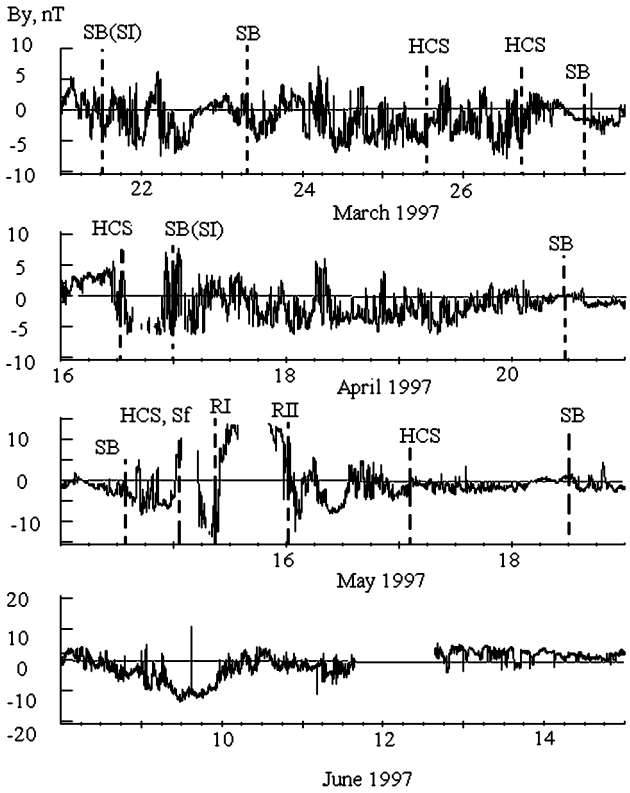

Figure 6. Dynamics of the IMF B_y component (the designations are the same as in Figure 3).

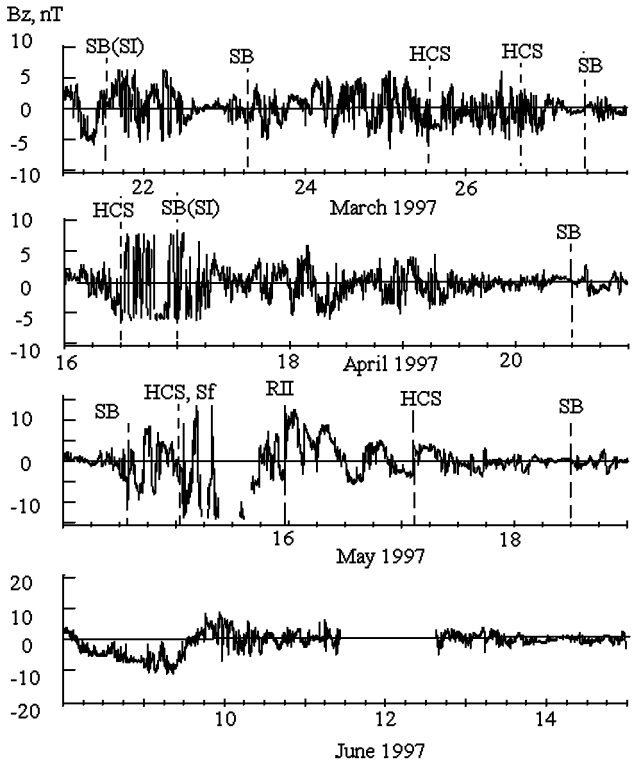

Figure 7. Dynamics of the IMF B_z component (the designations are the same as in Figure 3).

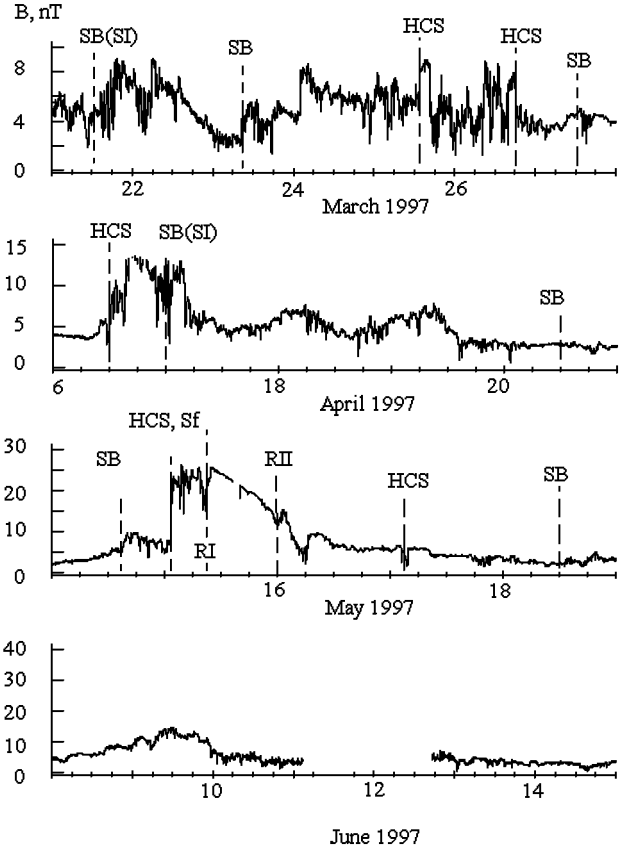

Figure 8. Dynamics of the IMF modulus (the designations are the same as in Figure 3).

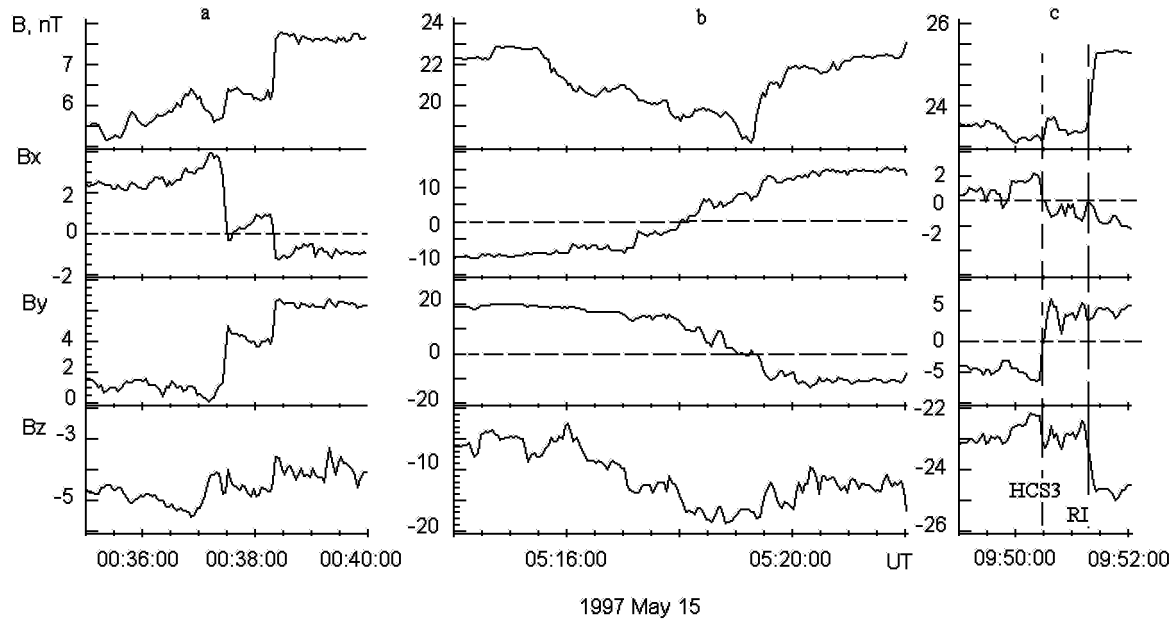

Figure 9. Variations of the 3-second mean values of the B, B_x, B_y, and B_z components of IMF according to the measurements on board the Wind satellite (courtesy of R. Lepping and CDA Web team): (a) the transition of HCS1 from the negative to the positive sector of IMF; (b) the return transition HCS2 from the positive to the negative sector; (c) a sequence of the HCS3 transitions from the negative to the positive sector and crossing the magnetic cloud boundary R_I.

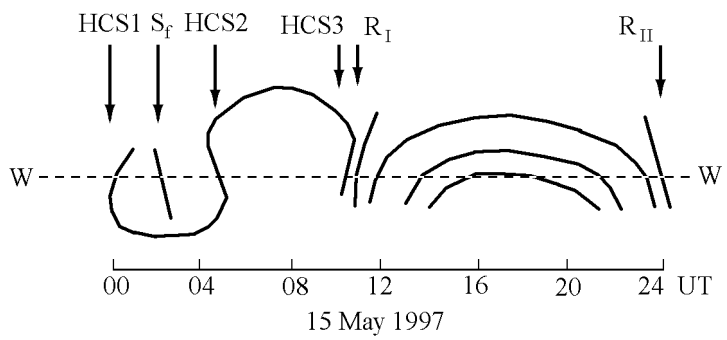

Figure 10. A scheme of the structure and configuration of the near-Earth interplanetary disturbance of 15 May 1997 projected onto the ecliptic plane. The designations are the same as in Figure 3.

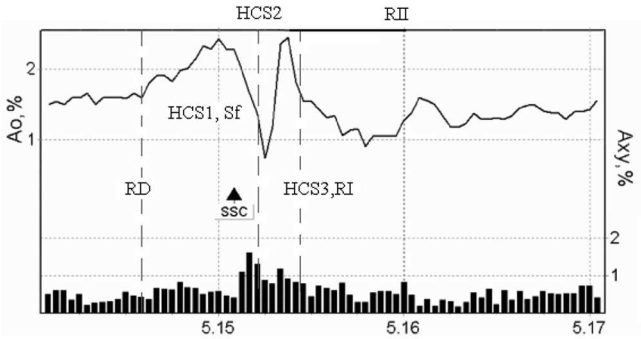

Figure 11. Variations of the galactic cosmic rays ($E \sim 10$ GeV) according to the neutron monitor data (A_0 and A_{xy} are the density and amplitude, respectively). Designations are the same as in Figure 3 and Table 2.